

HEAVY MAJORANA NEUTRINOS IN ELECTRON–POSITRON AND ELECTRON–PROTON COLLISIONS

W. BUCHMÜLLER and C. GREUB

Deutsches Elektronen Synchrotron DESY, Hamburg, Germany

Received 2 May 1991

Heavy Majorana neutrinos can be produced in charged and neutral current processes through their mixing with light neutrinos. We calculate production cross sections and final-state lepton spectra for e^+e^- annihilation and ep scattering, and compare the discovery potentials of present and future e^+e^- and ep colliders. At HERA heavy neutrinos with masses up to 160 GeV can be discovered, at LEP200 masses up to 190 GeV can be reached. The 500 GeV e^+e^- collider will probe for the first time heavy neutrino couplings to leptons of the second and third family. The most direct evidence for lepton number violation can be provided by ep colliders due to the nonzero lepton number of the initial state.

1. Introduction

The question of neutrino masses and lepton number violation [1] is a central problem of particle physics. In the standard model of strong and electroweak interactions neutrinos are exactly massless and, as a consequence, electron-, muon- and tau-number are conserved charges of the classical theory. In the quantum theory only three linear independent combinations, which one can form out of these lepton numbers and baryon number, are conserved because of the Adler–Bell–Jackiw anomaly involving the SU(2) gauge fields.

It is difficult to believe that the more fundamental theory, which contains the standard model as effective low-energy approximation, is also invariant under this global symmetry. In the simplest model of quark–lepton unification based on the group SU(5) only $B - L$, the difference of baryon and lepton number, is left as global symmetry up to a gravitational anomaly. If right-handed neutrinos are added to the fermions of the standard model one obtains a complete, anomaly-free SO(10) representation. The group SO(10) contains $B - L$ as U(1) subgroup which, due to the right-handed neutrinos, has no longer a gravitational anomaly and can now play the role of a spontaneously broken local symmetry. In most unified theories this is indeed the case, and at low energies one then obtains an extension of the standard model with right-handed neutrinos whose Majorana masses reflect the spontaneous breaking of $B - L$. A more complicated pattern with similar features emerges if one considers embeddings into the gauge group E_6 .

What are the observable consequences of heavy Majorana neutrinos? First of all they lead, via the see-saw mechanism [2], to small Majorana masses for electron-, muon- and tau-neutrinos and, hence, to processes which violate these lepton numbers, such as neutrino oscillations, $\mu \rightarrow e\gamma$, neutrinoless double- β decay, etc. The rates for these processes depend on masses and mixings of the light neutrinos, which are determined by the Majorana mass matrix of the right-handed neutrinos and the Dirac mass matrix which connects left- and right-handed neutrinos.

If the vacuum expectation value, which breaks $B - L$, is much smaller than the unification mass scale Λ_{GUT} , it is conceivable that the heavy Majorana neutrinos can be directly produced in collider experiments. In this case one would also expect an additional Z' vector boson with mass much smaller than Λ_{GUT} .

In the following we shall study in detail production and decays of heavy Majorana neutrinos in electron-positron and electron-proton scattering, which in part has already been discussed in ref. [3]. This will lead to a determination of the range of masses and mixings which can be explored with present and future e^+e^- and ep colliders.

The production of heavy neutral leptons has already been discussed in the literature [4–7]. The early analyses [4, 5] considered only the case of small center-of-mass energy, i.e. $\sqrt{s} \ll m_W, m_Z$, whereas in the more recent papers [6, 7] the full contribution of the Z resonance as well as possible effects from additional heavy vector bosons [7] are taken into account. In this paper we are interested in the production of a single heavy Majorana neutrino which, for e^+e^- annihilation, involves the interference of different charged current and neutral current processes. To our knowledge this case has not been discussed in the literature. The electroproduction of Majorana neutrinos is similar to the production of heavy Dirac leptons which was studied in refs. [8, 9].

The paper is organized as follows: in sect. 2 we describe the standard model with right-handed neutrinos, determine masses and mixings in charged and neutral currents, and evaluate branching ratios of the heavy neutrinos into different final states. In sect. 3 we then discuss electron-positron scattering with particular emphasis on the important t -channel processes, and sect. 4 deals with heavy neutrino production in electron-proton scattering. In sect. 5 we compare our model with other theories containing additional fermions and new currents, which occur in extended gauge theories. We summarize our results in sect. 6. Appendix A contains examples of mass matrices, which illustrate our assumptions on neutrino masses and mixings.

2. Standard model with right-handed neutrinos

“Right-handed neutrinos” ν_R are Weyl fermions whose $SU(3) \times SU(2) \times U(1)$ quantum numbers are defined through the Yukawa coupling term $\hat{l}\varphi\nu_R$, where $l = (\nu_L, e_L^-)$ is a lepton doublet and φ is the doublet of Higgs fields, i.e.

$\varphi = (\varphi^0, \varphi^-)$. Since l and φ have the same hypercharge ν_R is a gauge singlet. Hence Majorana mass terms for ν_R are allowed and the most general renormalizable, gauge-invariant lagrangian for the fields l , φ and ν_R reads

$$\mathcal{L}_\nu = \bar{l}i\not{D}l + \bar{\nu}_R i\not{\partial}\nu_R - \bar{l}\varphi g_\nu \nu_R - \bar{\nu}_R g_\nu^\dagger \varphi^\dagger l - \frac{1}{2}(\bar{\nu}_R m \nu_R^c + \bar{\nu}_R^c m^\dagger \nu_R). \quad (1)$$

Here g_ν and m are complex 3×3 matrices with $m = m^T$.

After spontaneous symmetry breaking one gets the Dirac mass matrix $m_D = g_\nu v$, where $v = \langle \varphi^0 \rangle_0 = 174$ GeV, in addition to the Majorana mass matrix m , and the neutrino mass eigenstates are obtained from the weak eigenstates of eq. (1) by means of unitary transformations on the fields ν_R and ν_L . The transformation of the ν_R can be used to choose the matrix m diagonal and real. The connection between the weak eigenstates ν_L, ν_R and the Majorana mass eigenstates ν, N can then be obtained as power series in $\xi = m_D(1/m)$ (assuming $\det(m_D) \ll \det(m)$, cf. e.g. [10]),

$$\nu = L + L^c, \quad N = R + R^c, \quad (2)$$

where

$$\nu_L = L + \xi R^c - \frac{1}{2}\xi\xi^\dagger L + \dots, \quad (3)$$

$$\nu_R = R - \xi^T L^c - \frac{1}{2}\xi^T \xi^* R + \frac{1}{2}\left(\xi^T \xi^* \xi^T + \frac{1}{m}\xi^\dagger \xi m_D^T\right)L^c + \dots \quad (4)$$

ν and N are the Majorana mass eigenstates, i.e.

$$\mathcal{L}_\nu = \frac{1}{2}\bar{\nu}(i\not{\partial} - m_\nu)\nu + \frac{1}{2}\bar{N}(i\not{\partial} - m_N)N + \mathcal{O}\left(\frac{1}{m^3}\right), \quad (5)$$

where

$$m_N = m + \mathcal{O}\left(\frac{1}{m}\right), \quad (6)$$

$$m_\nu = -m_D \frac{1}{m} m_D^T + \mathcal{O}\left(\frac{1}{m^3}\right). \quad (7)$$

The requirement that m_ν be diagonal and real fixes the unitary transformation on the weak eigenstates ν_L . In general the mass matrix m_l of the charged leptons is also complex and has to be diagonalized by a bi-unitary transformation. In the basis where m_ν is diagonal the unitary transformation on the charged left-handed leptons yields the usual Kobayashi–Maskawa (KM) type mixing matrix V in the leptonic part of the charged current.

In order to obtain charged and neutral currents in terms of mass eigenstates one has to insert the expansion (3) into the lagrangian (1). This yields

$$\mathcal{L}_1 = -J_{\text{NC}}^\mu Z_\mu - J_{\text{CC}}^\mu W_\mu^- - J_{\text{CC}}^{\mu\dagger} W_\mu^+, \quad (8)$$

where

$$J_{\text{NC}}^\mu = \frac{g}{2 \cos \theta_w} \left[\bar{\nu} (1 - \xi \xi^\dagger) \gamma^\mu \frac{1 - \gamma_5}{2} \nu + \bar{\nu} \xi \gamma^\mu \frac{1 - \gamma_5}{2} N \right. \\ \left. + \bar{N} \xi^\dagger \gamma^\mu \frac{1 - \gamma_5}{2} \nu + \bar{N} \xi^\dagger \xi \gamma^\mu \frac{1 - \gamma_5}{2} N + \mathcal{O}\left(\frac{1}{m^3}\right) \right], \quad (9)$$

$$J_{\text{CC}}^\mu = \frac{g}{\sqrt{2}} \left[\bar{e} V (1 - \frac{1}{2} \xi \xi^\dagger) \gamma^\mu \frac{1 - \gamma_5}{2} \nu + \bar{e} V \xi \gamma^\mu \frac{1 - \gamma_5}{2} N + \mathcal{O}\left(\frac{1}{m^3}\right) \right]. \quad (10)$$

Here V is the Kobayashi–Maskawa matrix of the lepton sector.

Production cross sections for the heavy neutrinos N_i will depend on the masses m_{N_i} and the mixings ξ_{ij} . Constraints from low-energy experiments typically yield $|\xi| < 0.1$ [11]. In this paper we will essentially determine the range of masses m_{N_i} which can be explored with present and future e^+e^- and ep colliders for mixings $|\xi|$ between 10^{-3} and 0.1. Such mixings are compatible with masses m_{N_i} in the hundred GeV range and also with the small masses m_{ν_i} bounded from above by experiment. Explicit examples of mass matrices m_D and m , which yield such masses and mixings, are given in appendix A.

Majorana neutrinos N_i with mixings $\xi^2 > 10^{-3}$ have to be heavier than the Z-boson since otherwise they would have already been produced in Z decays. The width of such heavy neutrinos is dominated by the two-body decays $N \rightarrow \ell^\pm W^\mp$ and $N \rightarrow \nu Z$. The corresponding partial widths are

$$\Gamma(N \rightarrow \ell^\pm W^\mp) = \frac{|(V\xi)_{\ell N}|^2}{8\sqrt{2}\pi} \frac{G_F}{m_N^3} (m_N^2 + 2m_W^2)(m_N^2 - m_W^2)^2, \quad (11)$$

$$\Gamma(N \rightarrow \nu_\ell Z) = \frac{|\xi_{\nu_\ell N}|^2}{8\sqrt{2}\pi} \frac{G_F}{m_N^3} (m_N^2 + 2m_Z^2)(m_N^2 - m_Z^2)^2. \quad (12)$$

For $V=1$ both widths are equal if phase space suppression can be ignored and one obtains

$$\Gamma(N \rightarrow \ell^- W^+) \equiv \Gamma_0 = 26 \text{ MeV} \left(\frac{|\xi_{\nu N}|}{0.1} \right)^2 \left(\frac{m_N}{200 \text{ GeV}} \right)^3. \quad (13)$$

The branching ratios into specific final states strongly depend on the flavour structure of the mixing matrix $\xi_{\nu_i N_j}$. However, one always has

$$\sum_l \text{BR}(N \rightarrow \nu_l Z) = \frac{1}{3}. \tag{14}$$

The branching ratio into the experimentally cleanest final states $e^\pm W^\mp (\rightarrow 2 \text{ jets})$ or $\mu^\pm W^\mp (\rightarrow 2 \text{ jets})$ is determined by the relative strength of the coupling $(V\xi)_{\tau N}$ of the heavy neutrino to the τ -lepton.

Via the see-saw mechanism large Majorana masses of a few hundred GeV may induce Majorana masses for the light neutrinos larger than 100 eV. Such neutrinos have to decay sufficiently fast in order to be cosmologically acceptable (for a review see ref. [12]). Theoretically favoured is the “invisible” decay mode $\nu \rightarrow \nu_e G$ [10, 13, 14], where G is some (pseudo) Goldstone boson. One may also worry that Majorana masses above 1 eV imply that any baryon asymmetry of the universe is washed out [15]. However, this can be avoided if the neutrino masses arise from spontaneous symmetry breaking and lepton number violating processes are sufficiently suppressed at high temperature (cf. ref. [10]). Hence, Majorana neutrino masses in the hundred GeV range are a viable, theoretically interesting possibility, which can be experimentally tested at present and future colliders.

3. Electron-positron annihilation

Given the expressions (9) and (10) for neutral and charged currents it is straightforward to compute the cross section for the production of a single heavy Majorana neutrino. From the s - and t -channel contributions shown in fig. 1 one

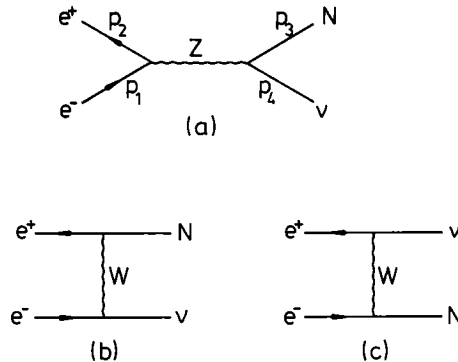


Fig. 1. Production of a single heavy Majorana neutrino through neutral (a) and charged (b, c) currents.

obtains the differential cross section

$$\begin{aligned} \frac{d\sigma}{dt} = \frac{G_F^2 m_W^4}{2\pi s^2} & \left[|\xi_{\nu N}|^2 \tan^4 \theta_W \frac{1}{(s - m_Z^2)^2} (t(t - m_N^2) + u(u - m_N^2)) \right. \\ & + \left| \frac{\xi_{\nu N}}{\cos^2 \theta_W} \left(\frac{1}{2} - \sin^2 \theta_W\right) \frac{1}{(s - m_Z^2)} - \frac{(V_\xi)_{eN} V_{e\nu}^*}{(t - m_W^2)} \right|^2 u(u - m_N^2) \\ & \left. + \left| \frac{\xi_{\nu N}}{\cos^2 \theta_W} \left(\frac{1}{2} - \sin^2 \theta_W\right) \frac{1}{(s - m_Z^2)} - \frac{(V_\xi)_{eN} V_{e\nu}^*}{(u - m_W^2)} \right|^2 t(t - m_N^2) \right]. \quad (15) \end{aligned}$$

Here

$$s = (p_1 + p_2)^2, \quad t = (p_1 - p_4)^2, \quad u = (p_2 - p_4)^2 \quad (16)$$

are the usual Mandelstam variables. One can sum over the light neutrinos in the final state since they cannot be experimentally distinguished.

Integrating $d\sigma/dt$ over the kinematically allowed range from $-(s - m_N^2)$ to 0 yields the total cross section

$$\begin{aligned} \sigma = \frac{G_F^2 m_W^4}{\pi s^2} & \left[\frac{1}{6} \frac{|\xi_{\nu N}|^2}{\cos^4 \theta_W} \frac{(\frac{1}{4} - \sin^2 \theta_W + 2 \sin^4 \theta_W)}{(s - m_Z^2)^2} (s - m_N^2)^2 (2s + m_N^2) \right. \\ & - \frac{\text{Re}(\xi_{\nu N} (V_\xi)_{eN}^* V_{e\nu})}{\cos^2 \theta_W} \frac{(1 - 2 \sin^2 \theta_W)}{(s - m_Z^2)} \\ & \times \left(\frac{3}{2} (s - m_N^2)^2 + (s - m_N^2)(m_N^2 + m_W^2) \right. \\ & \left. - (s + m_W^2)(s + m_W^2 - m_N^2) \log \frac{s + m_W^2 - m_N^2}{m_W^2} \right) \\ & + |(V_\xi)_{eN} V_{e\nu}^*|^2 \left((s - m_N^2) \left(\frac{s + 2m_W^2}{m_W^2} \right) \right. \\ & \left. - (2s + 2m_W^2 - m_N^2) \log \frac{s + m_W^2 - m_N^2}{m_W^2} \right) \left. \right]. \quad (17) \end{aligned}$$

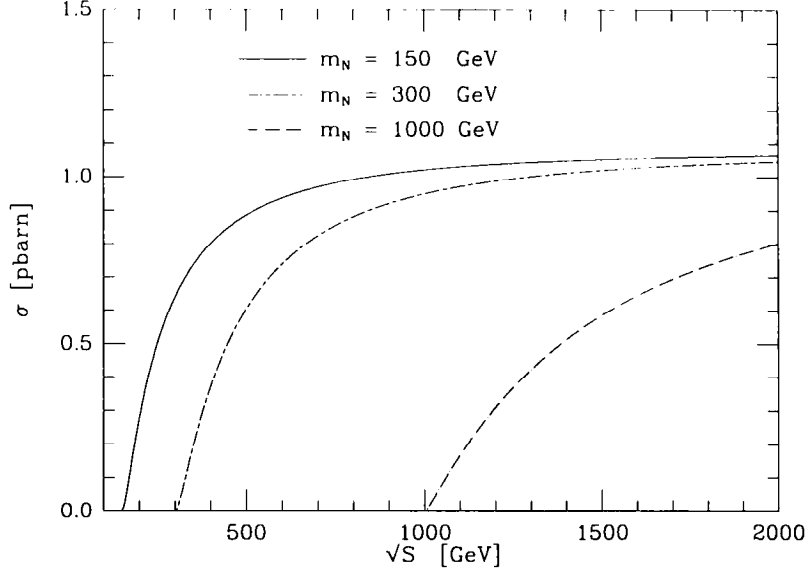


Fig. 2. Total cross section for the reaction $e^+e^- \rightarrow N\nu$ as function of the center-of-mass energy \sqrt{s} for three different heavy neutrino masses and $(V\xi)_{cN}V_{e\nu}^* = \xi_{\nu N} = 0.1$.

Due to the t -channel contributions (cf. figs. 1b,c) the cross section approaches asymptotically the constant

$$\sigma_\infty = \frac{1}{\pi} G_F^2 m_W^2 |(V\xi)_{cN}V_{e\nu}^*|^2. \quad (18)$$

Fig. 2 shows the cross section (17) for three different neutrino masses, $m_N = 150$ GeV, $m_N = 300$ GeV and $m_N = 1000$ GeV, $(V\xi)_{cN}V_{e\nu}^* = 0.1$ and $\xi_{\nu N} = 0.1$ as function of the center-of-mass energy up to $\sqrt{s} = 2000$ GeV. For comparison in fig. 3 the analogous cross sections are plotted with $\xi_{\nu N} = 0.1$ and $(V\xi)_{cN}V_{e\nu}^* = 0$. Obviously the t -channel contributions dominate over the entire range in \sqrt{s} by a factor between $\sim 10^2$ and $\sim 10^4$!

Fig. 4 shows the angular distribution $d\sigma/d\cos\theta$ of the produced heavy neutrino for $\sqrt{s} = 200$ GeV and $m_N = 100$ GeV and $m_N = 150$ GeV according to the differential cross section (15). The angle θ between the electron and the heavy neutrino is related to t by

$$t = -\frac{1}{2}(s - m_N^2)(1 + \cos\theta). \quad (19)$$

The angular distribution is forward-backward symmetric. The smaller the mass of the heavy neutrino, the more the cross section is peaked in the forward and backward direction.

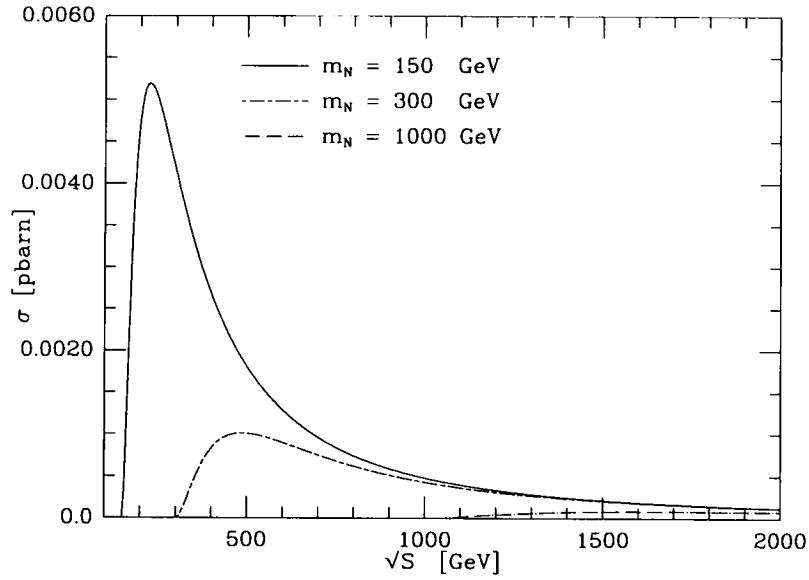


Fig. 3. Cross section for the process $e^+e^- \rightarrow Z N \nu$ as function of the center-of-mass energy \sqrt{s} for three different heavy neutrino masses and $(V\xi)_{cN}V_{c\nu}^* = 0$ and $\xi_{\nu N} = 0.1$.

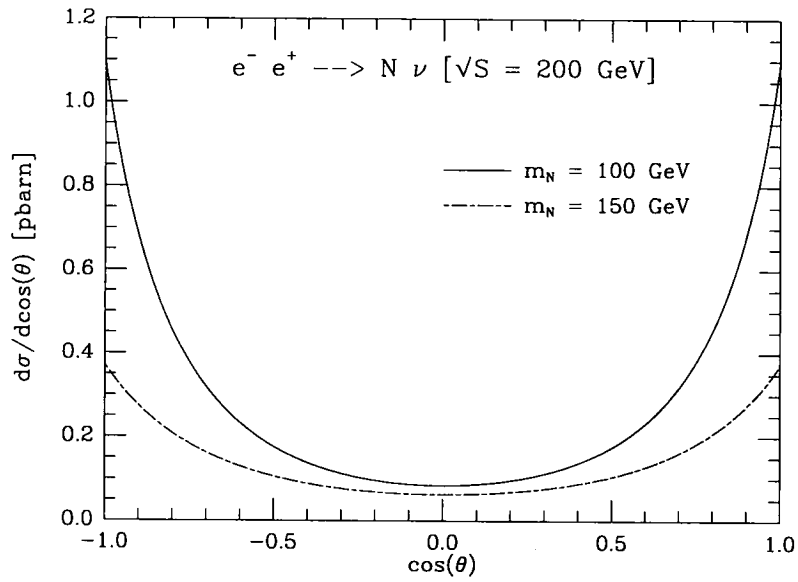
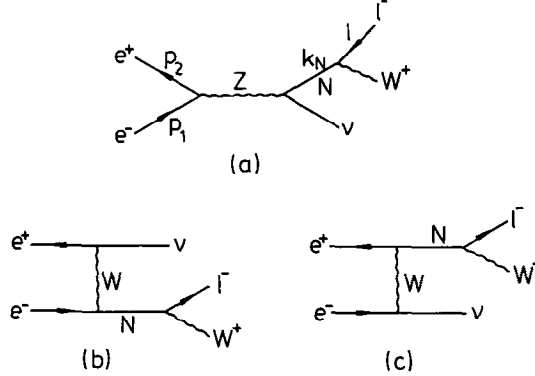


Fig. 4. Angular distribution of the produced heavy neutrino ($(V\xi)_{cN}V_{c\nu}^* = \xi_{\nu N} = 0.1$).


 Fig. 5. Neutral and charged current contributions to the reaction $e^+e^- \rightarrow \nu N (\rightarrow \ell^- W^+)$.

The heavy neutrinos predominantly decay into charged lepton and W-boson which further decays into two jets or a lepton pair. These are rather spectacular events, especially since the light neutrino, which is produced together with the heavy neutrino, escapes undetected. The decay amplitude is given by the three graphs depicted in fig. 5, which we have evaluated in the narrow-width approximation of the heavy neutrino propagator (cf. eq. (13)). A straightforward calculation yields the differential cross section in the variables of the final-state lepton (cf. fig. 5),

$$\begin{aligned}
 \frac{d\sigma}{dl_{\perp} dy_{\ell} dt} &= \frac{G_F^2 m_W^6 m_N^2 \text{BR}(N \rightarrow \ell W)}{4\pi^2 s^2 (m_N^2 - m_W^2)^2 (m_N^2 + 2m_W^2) m_{\perp}(k_N)} \\
 &\times \left[\cosh(y_N - y_{\ell}) - \frac{m_N^2 - m_W^2 - 2l_{\perp} k_{N\perp}}{2m_{\perp}(k_N)l_{\perp}} \right]^{-1/2} \\
 &\times \left[\frac{m_N^2 - m_W^2 + 2l_{\perp} k_{N\perp}}{2m_{\perp}(k_N)l_{\perp}} - \cosh(y_N - y_{\ell}) \right]^{-1/2} \\
 &\times \left\{ \left| \frac{\xi_{\nu N}}{s - m_Z^2} \frac{(\frac{1}{2} - \sin^2 \theta_W)}{\cos^2 \theta_W} - \frac{(V\xi)_{eN} V_{e\nu}^*}{(u - m_W^2)} \right|^2 A \right. \\
 &\left. + \left| \frac{\xi_{\nu N}}{s - m_Z^2} \frac{(\frac{1}{2} - \sin^2 \theta_W)}{\cos^2 \theta_W} - \frac{(V\xi)_{eN} V_{e\nu}^*}{(t - m_W^2)} \right|^2 B + \frac{|\xi_{\nu N}|^2}{(s - m_Z^2)^2} \tan^4 \theta_W C \right\},
 \end{aligned}
 \tag{20}$$

where

$$A = 8t \left[(m_N^2 - m_W^2)(t - m_N^2) + \left(m_N^2 - \frac{m_N^4}{2m_W^2} \right) \sqrt{s} l_\perp \exp(-y_\ell) \right], \quad (21)$$

$$B = \frac{4um_N^2}{m_W^2} \left[(m_N^2 - m_W^2)(u - m_N^2) + (m_N^2 - 2m_W^2) \sqrt{s} l_\perp \exp(y_\ell) \right], \quad (22)$$

$$C = 8u \left[(m_N^2 - m_W^2)(u - m_N^2) + \left(m_N^2 - \frac{m_N^4}{2m_W^2} \right) \sqrt{s} l_\perp \exp(y_\ell) \right] \\ + \frac{4tm_N^2}{m_W^2} \left[(m_N^2 - m_W^2)(t - m_N^2) + (m_N^2 - 2m_W^2) \sqrt{s} l_\perp \exp(-y_\ell) \right]. \quad (23)$$

Here l_\perp and y_ℓ are transverse momentum and rapidity of the lepton,

$$p_1 \cdot l = \frac{1}{2} \sqrt{s} l_\perp \exp(y_\ell), \quad p_2 \cdot l = \frac{1}{2} \sqrt{s} l_\perp \exp(-y_\ell), \quad (24)$$

k_N is the momentum of the heavy neutrino,

$$k_{N\perp} = \sqrt{\frac{tu}{s}}, \quad k_{NL} = \frac{t-u}{2\sqrt{s}}, \quad (25)$$

y_N and $m_\perp(k_N)$ are rapidity and transverse mass,

$$m_\perp(k_N) = (m_N^2 + k_{N\perp}^2)^{1/2}, \quad E_N = (m_\perp^2(k_N) + k_{NL}^2)^{1/2}, \\ y_N = \frac{1}{2} \log \frac{E_N + k_{NL}}{E_N - k_{NL}}. \quad (26)$$

Eq. (20) gives the differential cross section for the process $e^+e^- \rightarrow \nu N (\rightarrow \ell^- W^+)$. The cross section for the process $e^+e^- \rightarrow \nu N (\rightarrow \ell^+ W^-)$ is obtained through the interchange of u and t , and the substitution $y_\ell \rightarrow -y_\ell$ on the r.h.s. of eq. (20).

The differential cross section (20) can be numerically integrated over the variables y_ℓ and t in order to obtain the transverse momentum spectrum of the final-state leptons. From $k_N \cdot l = \frac{1}{2}(m_N^2 - m_W^2)$ one derives the kinematic limits

$$l_\perp \leq \frac{m_N^2 - m_W^2}{2m_N^2} \sqrt{s}, \quad (27)$$

$$\frac{m_N^2 - m_W^2 - 2l_\perp k_{N\perp}}{2m_\perp(k_N)l_\perp} \leq \cosh(y_N - y_\ell) \leq \frac{m_N^2 - m_W^2 + 2l_\perp k_{N\perp}}{2m_\perp(k_N)l_\perp}. \quad (28)$$

For fixed l_{\perp} this yields the lower limit on $k_{N\perp}$,

$$k_{N\perp} \geq k_{N\perp}^{\min} = \max \left\{ 0, \frac{4m_N^2 l_{\perp}^2 - (m_N^2 - m_W^2)^2}{4l_{\perp} (m_N^2 - m_W^2)} \right\}, \quad (29)$$

which, together with eq. (25), determines the allowed region of t ,

$$s - m_N^2 - \left((s - m_N^2)^2 - 4sk_{N\perp}^{\min 2} \right)^{1/2} \leq (-2t) \leq s - m_N^2 + \left((s - m_N^2)^2 - 4sk_{N\perp}^{\min 2} \right)^{1/2}. \quad (30)$$

Numerical integration of eq. (20) over the domain in y_l and t specified by eqs. (28) and (30) yields the differential cross section $d\sigma/dl_{\perp}$ plotted in fig. 6. The average transverse momentum is rather large, i.e. the final-state leptons will be well separated from the jets produced by the decaying W-boson. However, as fig. 6 shows, the actual value of $\langle l_{\perp} \rangle$ is strongly dependent on the difference between neutrino and W-boson mass. Contrary to the fully differential cross section (20), the transverse momentum spectrum $d\sigma/dl_{\perp}$ is identical for both reactions $e^+e^- \rightarrow \nu N$ ($\rightarrow \ell^{\pm} W^{\mp}$).

What are the implications of our results for the search of heavy neutrinos at future e^+e^- colliders? At LEP200 one expects an integrated luminosity of 500

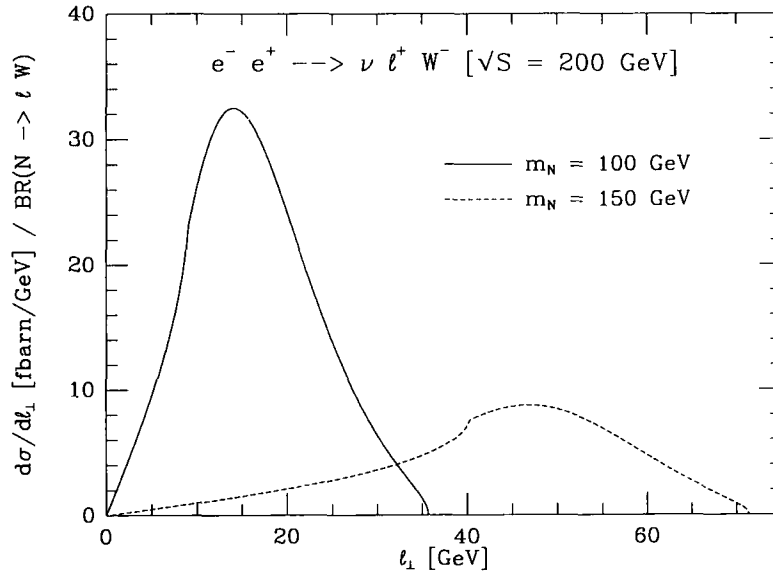


Fig. 6. Transverse momentum spectrum of final-state leptons.

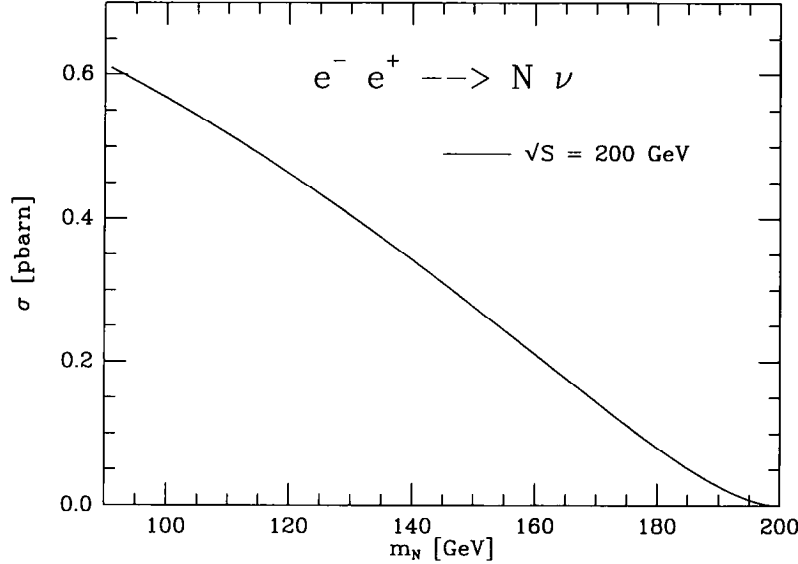


Fig. 7. Total cross section for the reaction $e^+ e^- \rightarrow N \nu$ as function of the neutrino mass ($(V\xi)_{eN} V_{e\nu}^* = \xi_{\nu N} = 0.1$).

pb^{-1} per year. The requirement of 10 heavy neutrino events then corresponds to a minimum cross section of 0.02 pb. Fig. 7 shows the production cross section $\sigma_{W,Z}$ for $(V\xi)_{eN} V_{e\nu}^* = \xi_{\nu N} = 0.1$ at $\sqrt{s} = 200$ GeV as function of the neutrino mass m_N . The cross section σ_Z for $(V\xi)_{eN} V_{e\nu}^* = 0$, $\xi_{\nu N} = 0.1$, is plotted in fig. 8. A rough approximation to both cross sections is ($100 \text{ GeV} < m_N < 200 \text{ GeV}$)

$$\sigma_{W,Z}(m_N) \approx \left(1 - \frac{m_N}{200 \text{ GeV}}\right) \text{pb} \approx 50 \sigma_Z(m_N). \quad (31)$$

From fig. 7 we conclude that the discovery limit at LEP200 is $m_N \approx 190$ GeV for $[(V\xi)_{eN} V_{e\nu}^*]^2 = 10^{-2}$ and $m_N \approx 160$ GeV for $[(V\xi)_{eN} V_{e\nu}^*]^2 = 10^{-3}$. The cross section σ_Z , which corresponds to the case $(V\xi)_{eN} V_{e\nu}^* = 0$, $\xi_{\nu N} = 0.1$, is not large enough to produce enough events if $m_N > 100$ GeV. This is unfortunate since the production via the Z-boson is equally sensitive to mixings with neutrinos of all three families. Hence σ_Z would be the dominant process in a case like $(V\xi)_{eN} V_{e\nu}^* \approx \xi_{\nu eN} \ll \xi_{\nu \tau N}$.

Plans for 500 GeV linear colliders aim at an integrated luminosity of 10 fb^{-1} per year. Hence a production cross section of 1 fb should be sufficient to discover a heavy neutrino. From fig. 2 we conclude that for $[(V\xi)_{eN} V_{e\nu}^*]^2 = 10^{-2}$ heavy neutrinos can be produced essentially up to the kinematic limit. For a 300 GeV neutrino one is sensitive down to $[(V\xi)_{eN} V_{e\nu}^*]^2 \approx 2 \times 10^{-5}$! Furthermore, as fig. 3 shows, due to the larger luminosity compared to LEP200, there will be about 10 neutrinos of 300 GeV mass produced via the Z-boson. Hence one is now also sensitive to the very interesting mixings $\xi_{\nu \mu N}$ and $\xi_{\nu \tau N}$.

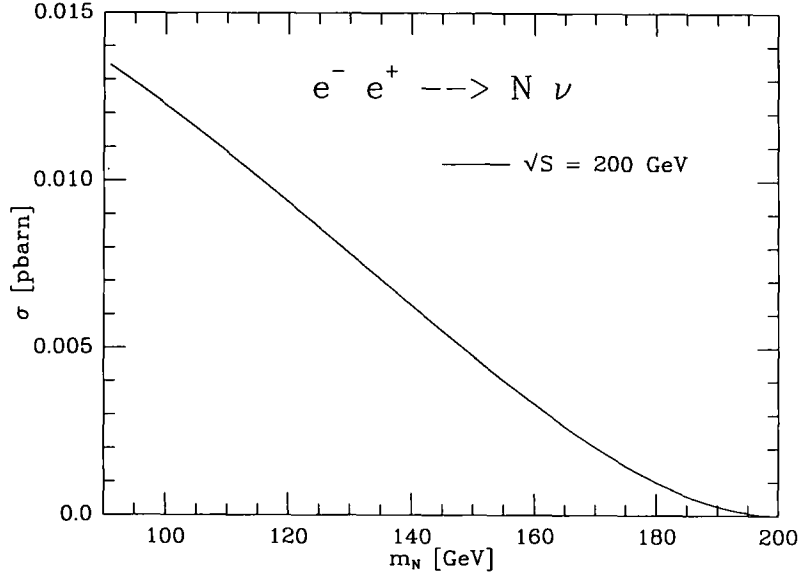


Fig. 8. Cross section for the process $e^+e^- \rightarrow N\nu$ as function of the neutrino mass ($(V\xi)_{eN}V_{e\nu}^* = 0$, $\xi_{\nu,N} = 0.1$).

At e^+e^- colliders it will be difficult to distinguish Majorana neutrinos from Dirac neutrinos since in both cases there will be an equal number of events with positively and negatively charged leptons in the final state. In order to distinguish Majorana from Dirac neutrinos one has to study for example the angular distribution of the heavy neutrinos, which we will discuss in more detail in sect. 5.

4. Electron–proton scattering

An advantage of ep scattering compared to e^+e^- annihilation is the nonvanishing lepton number L of the initial state. Production and decay of Dirac neutrinos leads only to $\Delta L = 0$ processes whereas Majorana neutrinos yield $\Delta L = 0$ and $\Delta L = 2$ processes with equal rate. Contrary to e^+e^- annihilation in ep scattering already the opposite charge of the final-state lepton is a clear signal of lepton number violation.

Production and decay of heavy Majorana neutrinos proceeds through the charged current processes shown in fig. 9. The differential cross section is given by [3]

$$\frac{d\sigma}{dx dy} = \frac{G_F^2 |(V\xi)_{eN}|^2}{2\pi} \frac{m_W^4}{(y\hat{s} + m_W^2)^2} \left[(\hat{s} - m_N^2)(u(x, \mu^2) + c(x, \mu^2)) \right. \\ \left. + (1-y)(\hat{s}(1-y) - m_N^2)(\bar{d}(x, \mu^2) + \bar{s}(x, \mu^2)) \right], \quad (32)$$

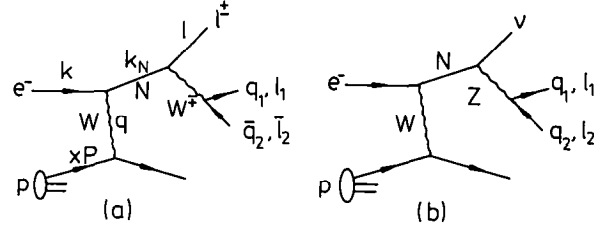


Fig. 9. Production and decay of heavy neutrinos in ep scattering.

where x , y and $\hat{s} = xs$ are the usual kinematic variables (cf. fig. 9),

$$s = (P + k)^2, \quad Q^2 = -q^2, \quad x = \frac{Q^2}{2P \cdot q}, \quad y = \frac{P \cdot q}{P \cdot k}, \quad (33)$$

which are restricted to the intervals

$$\frac{m_N^2}{s} \leq x \leq 1, \quad 0 \leq y \leq 1 - \frac{m_N^2}{xs}. \quad (34)$$

u , c , d and s are the densities of up, charm, down and strange quarks in the proton, which depend on the renormalization scale μ .

The total production cross section is obtained from eq. (32) after integration over x and y ,

$$\begin{aligned} \sigma = & \frac{|(V\xi)_{eN}|^2}{2\pi} G_F^2 m_W^2 \int_{m_N^2/s}^1 dx \left\{ \frac{(\hat{s} - m_N^2)^2}{\hat{s}(\hat{s} + m_W^2 - m_N^2)} (u(x, \mu^2) + c(x, \mu^2)) \right. \\ & \left. + \frac{1}{\hat{s}^2} \left[(\hat{s} - m_N^2)(\hat{s} + 2m_W^2) - m_W^2(2\hat{s} + 2m_W^2 - m_N^2) \log \frac{\hat{s} + m_W^2 - m_N^2}{m_W^2} \right] \right. \\ & \left. \times (\bar{d}(x, \mu^2) + \bar{s}(x, \mu^2)) \right\}. \quad (35) \end{aligned}$$

In fig. 10 the production cross section for heavy neutrinos is plotted as function of the neutrino mass m_N for three different values of the center-of-mass energy \sqrt{s} , which correspond to HERA ($\sqrt{s} = 314$ GeV), an upgraded version of HERA

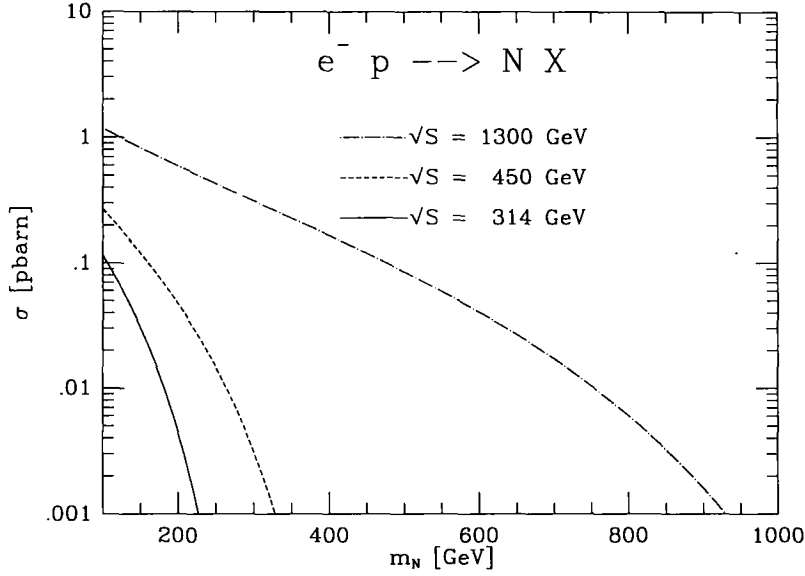


Fig. 10. Total cross section for the reaction $ep \rightarrow NX$ at $\sqrt{s} = 314$ GeV (HERA), $\sqrt{s} = 450$ GeV (HERA upgrade) and $\sqrt{s} = 1300$ GeV (LEP \otimes LHC) ($(V\xi)_{eN} = 0.1$).

($\sqrt{s} = 450$ GeV) and LEP \otimes LHC ($\sqrt{s} = 1300$ GeV) (cf. refs. [16, 17]). Here we have used set 1 of the Duke–Owens densities [18] with scales corresponding to the average transverse momentum of the produced heavy neutrino, i.e. $\mu^2 = 1000$ GeV 2 ($\sqrt{s} = 314$ GeV), $\mu^2 = 2000$ GeV 2 ($\sqrt{s} = 450$ GeV) and $\mu^2 = 4900$ GeV 2 ($\sqrt{s} = 1300$ GeV). The design luminosities of these machines are 2×10^{31} cm $^{-2}$ s $^{-1}$, 4×10^{32} cm $^{-2}$ s $^{-1}$ and 2×10^{32} cm $^{-2}$ s $^{-1}$, which, after one year of running, correspond to 200 pb $^{-1}$, 4000 pb $^{-1}$ and 2000 pb $^{-1}$, respectively. Requiring 5 events we then obtain from fig. 10 the discovery limits ($(V\xi)_{eN} = 0.1$) $m_N = 160$ GeV (HERA), $m_N = 320$ GeV (HERA upgrade) and $m_N = 870$ GeV (LEP \otimes LHC). This discovery limit for HERA is compatible with the results obtained in ref. [9] for mirror neutrinos.

The heavy neutrinos decay into the final states $\ell^\pm W^\mp$ and νZ with branching ratios discussed in sect. 2. The transverse momentum spectrum of the final-state lepton can be computed as for e^+e^- annihilation. The kinematic limits for the transverse momentum and rapidity are again given by eqs. (27) and (28). Transverse and longitudinal momentum of the heavy neutrino are determined by the electron energy E_e , the proton energy E_p , x and y ,

$$k_{N\perp} = ((1-y)y\hat{s} - ym_N^2)^{1/2}, \quad k_{NL} = xyE_p - (1-y)E_e + \frac{m_N^2}{4E_e}. \quad (36)$$

Together with eqs. (28) and (29) this yields the kinematic limits for x and y ,

$$\frac{1}{s} (k_{N\perp}^{\min} + m_{\perp}(k_{N\perp}^{\min}))^2 \leq x \leq 1, \quad (37)$$

$$\frac{\hat{s} - m_N^2 - \sqrt{(\hat{s} - m_N^2)^2 - 4\hat{s}k_{N\perp}^{\min 2}}}{2\hat{s}} \leq y \leq \frac{\hat{s} - m_N^2 + \sqrt{(\hat{s} - m_N^2)^2 - 4\hat{s}k_{N\perp}^{\min 2}}}{2\hat{s}}, \quad (38)$$

where $m_{\perp}(k_N)$ is the transverse momentum of the heavy neutrino (cf. eq. (26)).

The differential cross sections $d\sigma^{--}$ for the process $e^-p \rightarrow N (\rightarrow e^-W^+)X$ and $d\sigma^{-+}$ for the process $e^-p \rightarrow N (\rightarrow e^+W^-)X$ read (cf. [3])

$$\begin{aligned} \frac{d\sigma^{-\mp}}{dx dy dl_{\perp} dy_{\ell}} &= \frac{G_{\text{F}}^2 |(V_{\xi})_{eN}|^2}{4\pi^2 \hat{s}} \frac{m_W^6}{(y\hat{s} + m_W^2)^2} \frac{m_N^2 \text{BR}(N \rightarrow e^{\mp}W^{\pm})}{(m_N^2 - m_W^2)^2 (m_N^2 + 2m_W^2)} \frac{1}{m_{\perp}(k_N)} \\ &\times \left[\cosh(y_N - y_{\ell}) - \frac{m_N^2 - m_W^2 - 2l_{\perp}k_{N\perp}}{2m_{\perp}(k_N)l_{\perp}} \right]^{-1/2} \\ &\times \left[\frac{m_N^2 - m_W^2 + 2l_{\perp}k_{N\perp}}{2m_{\perp}(k_N)l_{\perp}} - \cosh(y_N - y_{\ell}) \right]^{-1/2} \\ &\times \left[A^{-\mp} \cdot (u(x, \mu^2) + c(x, \mu^2)) + B^{-\mp} \cdot (\bar{d}(x, \mu^2) + \bar{s}(x, \mu^2)) \right], \end{aligned} \quad (39)$$

where

$$\begin{aligned} A^{--} &= 8\hat{s} \left((m_N^2 - m_W^2) \left(\hat{s} - \frac{m_N^4}{2m_W^2} \right) \right. \\ &\quad \left. - 2 \left(m_N^2 - \frac{m_N^4}{2m_W^2} \right) (xE_p \exp(-y_{\ell}) + E_e \exp(y_{\ell})) l_{\perp} \right), \end{aligned} \quad (40)$$

$$\begin{aligned} B^{--} &= 8(\hat{s}(1-y) - m_N^2) \left\{ \hat{s}(1-y)(m_N^2 - m_W^2) \right. \\ &\quad \left. - 2 \left(m_N^2 - \frac{m_N^4}{2m_W^2} \right) xE_p l_{\perp} \exp(-y_{\ell}) \right\}, \end{aligned} \quad (41)$$

$$\begin{aligned} A^{-+} &= \frac{4\hat{s}m_N^2}{m_W^2} \left\{ (\hat{s} - 2m_W^2)(m_N^2 - m_W^2) \right. \\ &\quad \left. - 2(m_N^2 - 2m_W^2)l_{\perp} (E_e \exp(y_{\ell}) + xE_p \exp(-y_{\ell})) \right\}, \end{aligned} \quad (42)$$

$$\begin{aligned} B^{-+} &= \frac{4(\hat{s}(1-y) - m_N^2)m_N^2}{m_W^2} \left\{ \hat{s}(1-y)(m_N^2 - m_W^2) \right. \\ &\quad \left. - 2(m_N^2 - 2m_W^2)xE_p l_{\perp} \exp(-y_{\ell}) \right\}. \end{aligned} \quad (43)$$

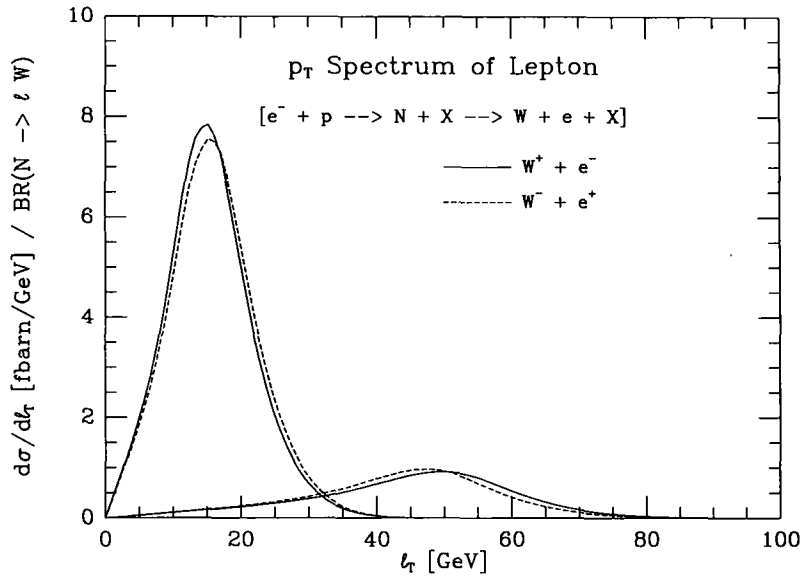


Fig. 11. Transverse momentum spectrum of the final-state leptons.

The transverse momentum spectrum of the final-state leptons can now be obtained by integrating eq. (39) over the variables y_ℓ , y and x in the intervals given by eqs. (28), (37) and (38). The differential cross sections for leptons with positive and negative charge are shown in fig. 11. The difference is small, but non-negligible. The integrated cross sections are equal by CP invariance. The average transverse momentum is strongly dependent on the difference between neutrino and W-boson mass.

Deep inelastic electron–nucleon scattering is an ideal process to discover lepton number violation, which can be achieved by simply measuring the charge of the final-state lepton. However, contrary to e^+e^- annihilation, heavy neutrinos can only be produced via the charged current, and hence only the electron – heavy neutrino coupling can be tested.

5. Other models

The crucial properties of the “standard model with right-handed neutrinos”, which we described in sect. 2, are the Majorana nature of light and heavy neutrinos and their couplings to W- and Z-bosons which follow from the structure of Dirac and Majorana mass matrices. Other models can differ from this “standard model” in the number of predicted heavy neutrinos, the realization of lepton number violation and the possible presence of additional currents, coupled to new heavy vector bosons.

E_6 models (cf. ref. [19]), for instance, predict three new neutrinos in addition to ν_R and ν_L for each family, two as part of isodoublets, and one more isosinglet, which appear in the 27-dimensional representation,

$$\begin{pmatrix} N \\ E^- \end{pmatrix}_L, \quad \begin{pmatrix} \tilde{N} \\ \tilde{E}^- \end{pmatrix}_R, \quad n. \quad (44)$$

Together with the doublet $(\nu, e^-)_L$ and the singlet ν_R one then obtains for three families a 15×15 neutrino mass matrix whose entries depend on the pattern in which E_6 is spontaneously broken to the standard model gauge group as well as on possible family symmetries. If lepton number is spontaneously broken the mass eigenstates are Majorana neutrinos; in the case of conserved lepton number one has Dirac neutrinos. Production cross sections and signatures of exotic E_6 particles in e^+e^- annihilation have been studied in detail in ref. [7].

The cross sections for the production of a single heavy Majorana neutrino in e^+e^- annihilation and ep scattering have been evaluated in sects. 3 and 4. For Dirac neutrinos there are some important differences due to the conservation of lepton number: in ep scattering the lepton charges in initial and final states are always equal, and in e^+e^- annihilation the angular distributions of heavy neutrinos with positive and negative lepton number are different.

The differential cross section for Dirac neutrinos with $L_N = L_{e^-}$ is determined by the processes shown in figs. 1a, c which give (cf. eq. (15))

$$\begin{aligned} \frac{d\sigma}{dt} = & \frac{G_F^2 m_W^4}{2\pi s^2} \left[|\xi_{\nu N}|^2 \tan^4 \theta_W \frac{1}{(s - m_Z^2)^2} u(u - m_N^2) \right. \\ & \left. + \left| \frac{\xi_{\nu N}}{2 \cos^2 \theta_W} \frac{(1 - 2 \sin^2 \theta_W)}{(s - m_Z^2)} - \frac{(V\xi)_{eN} V_{e\nu}^*}{(u - m_W^2)} \right|^2 t(t - m_N^2) \right]. \quad (45) \end{aligned}$$

The cross section for Dirac neutrinos with $L_N = L_{e^+}$ is obtained by interchanging the variables t and u on the r.h.s. of eq. (45). Hence neutrinos with $L_N = L_{e^-}$ are predominantly produced in the forward direction (with respect to the electron momentum), whereas neutrinos with $L_N = L_{e^+}$ are mostly emitted in the backward direction. The differential cross sections $d\sigma/d\cos\theta$ for Dirac neutrinos with $L_N = L_{e^-}$ and Majorana neutrinos are compared in figs. 12 and 13. The angle θ between the momenta of electron and heavy neutrino is related to the momentum transfer t according to eq. (19). Fig. 12 corresponds to the case $(V\xi)_{eN} V_{e\nu}^* = \xi_{\nu N} = 0.1$, where the W contribution dominates. The t - and u -channel exchanges yield the enhancements in forward and backward direction. For $(V\xi)_{eN} V_{e\nu}^* = 0$, $\xi_{\nu N} = 0.1$, which is plotted in fig. 13, one only has an s -channel contribution. Hence the

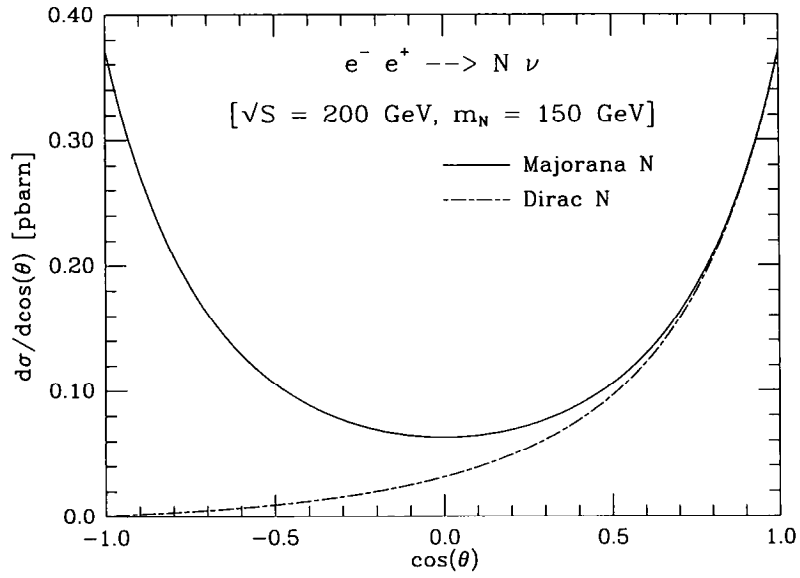


Fig. 12. Angular distribution of Dirac and Majorana neutrinos for W and Z exchange ($(V\xi)_{cN}V_{c\nu}^* = \xi_{\nu N} = 0.1$).

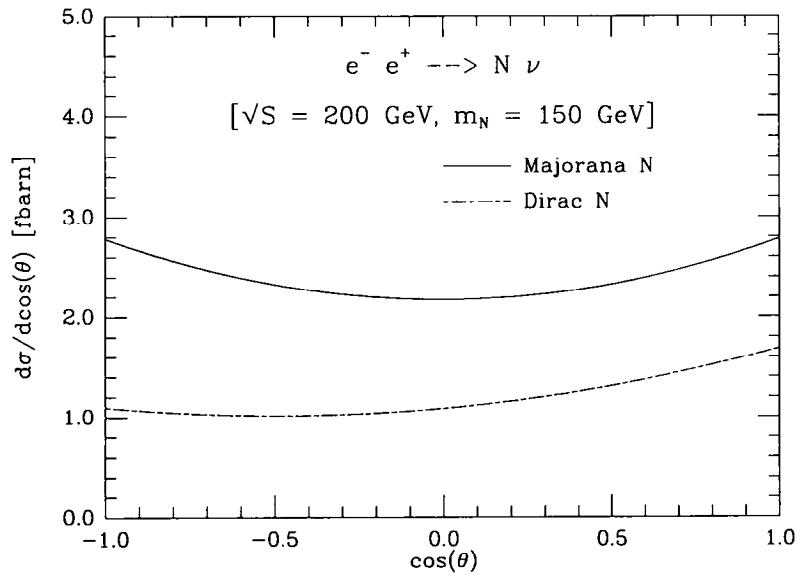


Fig. 13. Angular distribution of Dirac and Majorana neutrinos for Z exchange only ($(V\xi)_{cN}V_{c\nu}^* = 0, \xi_{\nu N} = 0.1$).

angular distribution is rather isotropic and it will be difficult to distinguish between Dirac and Majorana neutrinos.

The production cross section for heavy neutrinos can be enhanced compared to the “standard model” if there are additional vector bosons which couple to new currents. In the framework of unified theories the standard model gauge group $SU(3)_c \times SU(2)_L \times U(1)_Y$ may eventually be embedded into E_6 via the following chain:

$$\begin{aligned}
SU(3)_c \times SU(2)_L \times U(1)_Y &\subset SU(3)_c \times SU(2)_L \times U(1)_Y \times U(1)_{Y'} \times U(1)_E \\
&\subset SU(3)_c \times SU(2)_L \times SU(2)_R \times U(1)_{B-L} \times U(1)_E \\
&\subset SU(4)_{PS} \times SU(2)_L \times SU(2)_R \times U(1)_E \\
&\subset SO(10) \times U(1)_E \\
&\subset E_6.
\end{aligned} \tag{46}$$

At energies below 1 TeV only the additional gauge bosons corresponding to the first two embeddings can be relevant, i.e. the two neutral bosons of the $U(1)$ factors $U(1)_{Y'}$ and $U(1)_E$ and the W_R boson of $SU(2)_R \times U(1)_{B-L}/U(1)_Y \times U(1)_{Y'}$. In the extension to the Pati–Salam $SU(4)_{PS}$ leptoquarks appear which cause flavour-changing neutral currents and have hence to be heavier than 100 TeV, and the remaining generators in $SO(10)$ and E_6 lead to baryon number violating processes.

The simplest extension of the standard model is the addition of the $U(1)_{Y'}$ neutral vector boson contained in $SO(10)$. The standard model fermions together with the right-handed neutrinos form an anomaly-free representation of $SO(10)$. A general analysis of constraints on additional neutral vector bosons has recently been carried out by different groups [21, 22]. Using the simplest Higgs representation one obtains for its mass the lower bound [23]

$$m_{Z'} > 570 \text{ GeV}. \tag{47}$$

For the charged vector boson W_R lower bounds on the mass have been derived from various low-energy processes [24] which, however, all depend on certain assumptions such as the requirement of spontaneous parity breaking. For $g_R = g_L$, i.e. equal gauge couplings of W_L and W_R , a conservative lower bound on the W_R boson mass is $m_{W_R} > 300 \text{ GeV}$ [24].

Even if the vector bosons W_R and Z' should be too heavy to be directly produced at colliders considered in this paper, their unsuppressed couplings to right-handed neutrinos could yield rather large cross sections for pair production of Majorana neutrinos. Taking into account only the neutral vector boson Z' , the

relevant part of the interaction lagrangian is given by

$$\mathcal{L}_1 = -g' \sqrt{2/3} J'_{\text{NC}\mu} Z'^{\mu}, \quad (48)$$

$$J'_{\text{NC}}{}^{\mu} = \bar{e} \gamma^{\mu} \left(\frac{1}{2} - \frac{1}{4} \gamma_5 \right) e + \frac{5}{8} \bar{N} \gamma^{\mu} \gamma_5 N, \quad (49)$$

$$g'^4 = 32 m_{\text{W}}^4 G_{\text{F}}^2 \tan^4 \theta_{\text{W}}. \quad (50)$$

The coupling constants of the standard model $U(1)_{\text{Y}}$ and the additional $U(1)_{\text{Y}'}$ factor are related by the embedding into the unified gauge group $SO(10)$. For heavy Z' one obtains the pair production cross section

$$\sigma_{Z'}(e^+ e^- \rightarrow \text{NN}) = \frac{125 G_{\text{F}}^2 \tan^4 \theta_{\text{W}} m_{\text{W}}^4}{432 \pi m_{Z'}^4} s \beta^3, \quad s \ll m_{Z'}^2, \quad (51)$$

where

$$\beta = \sqrt{1 - 4m_{\text{N}}^2/s} \quad (52)$$

is the velocity of the heavy neutrinos. The β^3 factor in eq. (51) is due to the γ_5 coupling of the heavy neutrinos in the neutral current (49) which is a consequence of their Majorana nature. From eq. (51) we conclude that at $\sqrt{s} = 500$ GeV, with $m_{Z'} = 1$ TeV and an integrated luminosity of 10 fb^{-1} neutrinos with masses up to 200 GeV can be discovered. Via the standard model charged current the production of a single heavy neutrino with this mass is possible for mixings down to $[(V_{\xi})_{\text{eN}} V_{\text{e}\nu}^*]^2 \sim 10^{-5}$.

6. Summary

In the standard model neutrinos are massless, which is consistent with all currently available experimental data. However, the prevailing theoretical prejudice is that neutrinos are massive, and a natural explanation of the smallness of neutrino masses is provided by the see-saw mechanism. The light neutrinos ν_e , ν_{μ} and ν_{τ} are thereby related to heavy Majorana neutrinos whose masses are proportional to the scale of lepton number violation. This mass scale may be much larger than the Fermi scale of electroweak symmetry breaking, but it may also be below 1 TeV. This latter possibility is almost a necessity in extended gauge models which predict extra vector bosons with masses in the hundred GeV range.

In the previous sections we have discussed the production of a single heavy Majorana neutrino in e^+e^- annihilation and ep scattering, which proceeds via neutral and charged current processes due to the mixing of heavy and light neutrinos. An essential result of our analysis is the importance of the W exchange

processes in e^+e^- annihilation which, at a 500 GeV collider, allow to test for mixings down to $[(V\xi)_{eN}V_{e\nu}^*]^2 \sim 10^{-5}$ for a 300 GeV neutrino! Such a collider would also be sensitive to mixings with neutrinos of the second and third family $\xi_{\nu_\mu N}, \xi_{\nu_\tau N}$ of order 0.1.

The main advantage of ep colliders compared to e^+e^- colliders is the nonvanishing lepton number of the initial state. Hence, a violation of lepton number can be discovered just by measuring the charge of the final-state lepton. The same is true for the e^-e^- mode of a linear collider. On the contrary, in e^+e^- annihilation heavy Dirac and Majorana neutrinos can only be distinguished by their different angular distribution. For a mixing $(V\xi)_{eN} = 0.1$ the discovery limit is $m_N = 160$ GeV at HERA and reaches $m_N = 870$ GeV at LEP \otimes LHC!

In this paper we have focussed on the simplest model with heavy Majorana neutrinos, the standard model with one right-handed neutrino for each family. Most of our results can easily be applied to other models with more or less heavy neutrinos. Particularly interesting are extended gauge theories with additional neutral vector bosons, whose masses are related to the heavy neutrino masses. If the extra vector bosons are not too heavy the cross section for pair production of heavy neutrinos becomes important since the couplings of the new vector bosons to heavy neutrinos are not suppressed by small mixing angles.

In the coming years we can hope for important new experimental results on neutrino masses and mixings, especially from measurements of the solar neutrino flux. Complementary regions in parameter space will be probed in collider experiments, which could even lead to the discovery of heavy neutrinos!

Appendix A

In the previous sections we have studied production and decays of heavy Majorana neutrinos with masses in the hundred GeV range and mixings ξ in charged and neutral currents between 0.1 and 3×10^{-3} . One may wonder whether such a low mass scale of lepton number violation and such rather “large” mixings are compatible with experimental upper bounds on light neutrino masses and mixings. From the see-saw formula (7)

$$m_\nu = -m_D \frac{1}{m} m_D^T + \mathcal{O}\left(\frac{1}{m^3}\right)$$

one obtains $\det(m_\nu) = (\det(m_D))^2 / \det(m)$. For heavy Majorana neutrino masses of the order of the Fermi scale, i.e. $\det(m) = v^3$, where $v = 174$ GeV, the experimental upper limits $m_{\nu_e} < 18$ eV, $m_{\nu_\mu} < 0.25$ MeV, $m_{\nu_\tau} < 35$ MeV [25] imply $\det(m_D) < 9 \times 10^{-4}$ GeV³.

This is not too far from the determinant of the charged lepton mass matrix $\det(m_\ell) = m_e m_\mu m_\tau = 9 \times 10^{-5}$ GeV³. Hence Majorana neutrino masses in the hundred GeV range do not require unreasonably small Yukawa couplings.

In analogy to the Kobayashi–Maskawa matrix one might expect that mixings between light and heavy neutrinos are of order $\sqrt{m_\nu/m}$. For the electron neutrino this would yield $\xi_{ee} = \sqrt{m_{\nu_e}/m} < 10^{-5}$, which is much smaller than the mixings on which collider experiments will be sensitive. This naive expectation is indeed correct if the matrices m_D and m can be simultaneously diagonalized by unitary transformations on the field ν_L and ν_R . However, this is a strong assumption which may be very misleading, and one can easily construct examples with mixings $\xi_{ij} \gg \sqrt{m_{\nu_i}/m_j}$. In the following we present a three-family generalization of the two-family example discussed in ref. [10], which illustrates that one may have large mixings for arbitrarily small masses m_ν .

Let us write the Dirac mass matrix m_D as

$$m_D = m_D^{(0)} + \epsilon m_D^{(1)}, \quad \epsilon \ll 1, \tag{A.1}$$

and choose a basis for the gauge singlet neutrinos ν_R such that the majorana mass matrix is diagonal and real,

$$\frac{1}{m} = \begin{pmatrix} 1/M_1 & 0 & 0 \\ 0 & 1/M_2 & 0 \\ 0 & 0 & 1/M_3 \end{pmatrix}. \tag{A.2}$$

We now demand

$$m_\nu^{(0)} = -m_D^{(0)} \frac{1}{m} m_D^{(0)\text{T}} = 0, \tag{A.3}$$

which yields as general solution for $m_D^{(0)}$

$$m_D^{(0)\text{T}} = (v, \alpha v, \beta v), \tag{A.4}$$

where v is an arbitrary column vector.

Requiring m_ν to be diagonal and not identically vanishing to order ϵ one arrives at $\beta = 0$. For mass and mixing matrices one then finds

$$m_\nu = \epsilon \begin{pmatrix} \lambda + O(\epsilon) & 0 & 0 \\ 0 & -\alpha^2 \lambda + O(\epsilon) & 0 \\ 0 & 0 & \epsilon \kappa \end{pmatrix}, \tag{A.5}$$

$$\xi = \begin{pmatrix} m_1/M_1 & m_2/M_2 & m_3/M_3 \\ \alpha m_1/M_1 & \alpha m_2/M_2 & \alpha m_3/M_3 \\ 0 & 0 & 0 \end{pmatrix} + O(\epsilon). \tag{A.6}$$

Note that one of the neutrino masses is of order ϵ^2 . The parameters λ and κ in eq. (57) can be arbitrarily chosen. Together with the corrections of order ϵ to the matrix ξ this determines the matrix $m_D^{(1)}$ in eq. (53).

An amusing prediction of our example is a relation between the large mixing angles and the masses of the corresponding light neutrinos,

$$\left(\frac{\xi_{\nu_2 N_i}}{\xi_{\nu_1 N_i}} \right)^2 = - \frac{m_{\nu_2}}{m_{\nu_1}}. \quad (\text{A.7})$$

With $m_1 \sim 10$ GeV and $M_1 \sim 100$ GeV one would obtain $\xi_{\nu_1 N_1} \sim 0.1$, which is about the largest mixing compatible with charged current universality [11]. Our example illustrates that, due to the see-saw mechanism, neutrino masses and mixings may be very different from the patterns found in the quark mass matrices.

References

- [1] P. Langacker, *in* Neutrinos, ed. H.V. Klapdor (Springer, Berlin, 1988) p. 71
- [2] T. Yanagida, *in* Workshop on Unified theories, KEK report 79-18 (1979) p. 95;
M. Gell-Mann et al., *in* Supergravity, ed. P. van Nieuwenhuizen and D. Freedman (North-Holland, Amsterdam, 1979) p. 315
- [3] W. Buchmüller and C. Greub, Phys. Lett. B256 (1991) 465
- [4] J.D. Bjorken and C.H. Llewellyn Smith, Phys. Rev. D7 (1973) 887
- [5] A. Ali, Phys. Rev. D10 (1974) 2801
- [6] M. Gourdin and X.Y. Pham, Nucl. Phys. B164 (1980) 387
- [7] F. del Aguila, E. Laermann and P.M. Zerwas, Nucl. Phys. B297 (1988) 1
- [8] R.J. Cashmore et al., Phys. Rep. 122 (1985) 275
- [9] F. Csikor and I. Montvay, Phys. Lett. B231 (1989) 503;
F. Csikor, preprint DESY 90-073 (1990)
- [10] W. Buchmüller and D. Wyler, Phys. Lett. B249 (1990) 458
- [11] M. Gronau, C.N. Leung and J.L. Rosner, Phys. Rev. D29 (1984) 2539;
P. Langacker and D. London, Phys. Rev. D38 (1988) 886
- [12] E.W. Kolb and M.S. Turner, The early universe (Addison-Wesley, New York, 1990)
- [13] J. Schechter and J.W.F. Valle, Phys. Rev. D25 (1982) 774
- [14] M.C. Gonzalez-Garcia, A. Santamaria and J.W.F. Valle, Nucl. Phys. B342 (1990) 108
- [15] M. Fukugita and T. Yanagida, Phys. Rev. D42 (1990) 1285;
A.E. Nelson and M.S. Barr, Phys. Lett. B246 (1990) 141
- [16] J. Feltesse, *in* Proc. LHC Workshop, ed. G. Jarlskog and D. Rein, CERN 90-10 (1990) p. 219
- [17] R. Rückl, *in* Proc. LHC Workshop, ed. G. Jarlskog and D. Rein, CERN 90-10 (1990) p. 229
- [18] D. Duke and J.F. Owens, Phys. Rev. D30 (1984) 49
- [19] P. Langacker, Phys. Rep. 72 (1981) 185
- [20] J. Maalampi and M. Roos, Phys. Rep. 186 (1990) 53
- [21] G. Altarelli, R. Casalbuoni, F. Feruglio and R. Gatto, Phys. Lett. B245 (1990) 669
- [22] A. Chiappinelli, M. Consoli and C. Verzegnassi, preprint LAPP-TH-318/90 (1990)
- [23] W. Buchmüller, C. Greub and P. Minkowski, preprint DESY 91-053 (1991)
- [24] P. Langacker and S. Uma Sankar, Phys. Rev. D40 (1989) 1569
- [25] Review of Particle Properties, Phys. Lett. B239 (1990) 1